Olson, J. S., Mims, M. P., & Reisberg, P. I. (1982) in *Hemoglobin and Oxygen Binding* (Ho, C., Ed.) pp 393–398, Elsevier/North-Holland, New York.
Olson, J. S., McKinnie, R.-E., Mims, M. P., & White, D. K. (1983) *J. Am. Chem. Soc. 105*, 1522–1527.
Reisberg, P. C., & Olson, J. S. (1980a) *J. Biol. Chem. 255*, 4144–4150.
Reisberg, P. C., & Olson, J. S. (1980b) *J. Biol. Chem. 255*, 4151–4158.
Reisberg, P. C., & Olson, J. S. (1980c) *J. Biol. Chem. 255*, 4159–4169.
Rubinow, S. C., & Kassner, R. J. (1984) *Biochemistry 23*, 2590–2595.
Stetzkowski, F., Cassoly, R., & Banerjee, R. (1979) *J. Biol. Chem. 254*, 11351–11356.
St. George, R. C. C., & Pauling, L. (1951) *Science 114*, 629–634.
Taniguchi, S., & Kamen, M. D. (1963) *Biochim. Biophys. Acta 74*, 438–445.
Weber, P. C., Bartsch, R. G., Cusanovich, M. A., Hamlin, R. C., Howard, A., Jordon, S. R., Kamen, M. D., Meyer, T. E., Wertherford, D. U., Xuong, N. H., & Salemme, F. R. (1980) *Nature (London) 286*, 302–304.
Weber, P. C., Howard, A., Xuong, N. H., & Salemme, F. R. (1981) *J. Mol. Biol. 153*, 399–424.

Hysteresis and Conformational Drift of Pressure-Dissociated Glyceraldehydephosphate Dehydrogenase†

Kancheng Ruan and Gregorio Weber*
Department of Biochemistry, School of Chemical Sciences, University of Illinois, Urbana, Illinois 61801
Received September 30, 1988

ABSTRACT: Pressure dissociation of yeast glyceraldehydephosphate dehydrogenase (GAPDH) was studied by fluorescence spectroscopy. Observations in the range of −5 to 30 °C indicate that monomer association into the tetramer proceeds with an enthalpy change of −14 kcal mol^{-1} and a large increase in entropy which at 25 °C amounts to 18 kcal mol^{-1}. The large conformational drift and the low-temperature stability of the tetramer recovered after decompression facilitated a comparison of its properties with those of the native tetramer. Significant differences in absorption and fluorescence-excitation polarization spectra, yield of tryptophan fluorescence, and binding of anilinonaphthalenesulfonate and NADH were observed. At 0 °C the standard free energies of association of the monomers into the native and drifted tetramers were respectively −32 and −29 kcal mol^{-1}. The volume change upon association measured from the pressure span of the compression curves was 200–230 mL mol^{-1} but four times as large when derived from the displacement of the compression curves with total protein concentration. This large discrepancy can be explained by the existence in the native tetramer population of a distribution of free energies of association with a dispersion from the mean of about 6 kcal mol^{-1}. At 0 °C and 1 bar ATP and ADP decreased the stability of the GAPDH tetramer by changes in free energy of association of +3.7 and +4.1 kcal mol^{-1}, respectively. NAD and c-AMP stabilized it by −2.3 and −1.3 kcal mol^{-1}. The variation in sign and magnitude of the ligand-induced changes in free energy of association observed in this case, and previously in hexokinase [Ruan, K., & Weber, G. (1988) *Biochemistry 27*, 3295], and the heterogeneity of the free energy of association of GAPDH, revealed as indicated above, lead to the conclusion that oligomeric aggregates exist in a variety of conformations that depend upon the protein concentration, temperature, pressure, and the presence of specific ligands. The multiplicity of species revealed by the energetics raises questions about the significance of the structures of oligomeric proteins determined by X-ray crystallography.

Theory

The thermodynamic dissociation constant K of the reaction involving an equilibrium between tetramer and monomers is

$$K = 256a^4C^3/(1 - a) \quad (1)$$

where a is the degree of dissociation into monomers and C the protein concentration, as tetramer. For practical purposes K may be conveniently expressed as a protein concentration $C_{1/2}$ at which $a = 1/2$:

$$C_{1/2}{}^3 = (K/32) = 8a^4C^3/(1 - a) \quad (2)$$

The free energy[1] of monomer *association* into the tetramer is

$$\&G = RT \ln (32C_{1/2}{}^3) = RT(3.467 + 3 \ln C_{1/2}) \quad (3)$$

If $C_{1/2}$ and a_P, respectively, denote the half-dissociation concentration at atmospheric pressure and the degree of dissociation at pressure p

$$\ln (a_P{}^4/(1 - a_P)) = \ln (C_{1/2}/2C)^3 + p\&V/RT \quad (4)$$

and a plot of the left-hand side of eq 4 against the applied

† This research was supported by a grant from the National Institutes of Health (GM 11223) to G.W.

[1] Abbreviations: GAPDH, glyceraldehydephosphate dehydrogenase; ADP, adenosine 5′-diphosphate; ATP, adenosine 5′-triphosphate; c-AMP, cyclic adenosine 5′-monophosphate; NAD and NADH, oxidized and reduced nicotinamide adenine dinucleotide; Tris, tris(hydroxymethyl)-aminomethane; ANS, 1-anilino-8-naphthalenesulfonate; 2,5-DNS, 2-(dimethylamino)-5-naphthalenesulfonyl chloride; EDTA, ethylenediaminetetraacetic acid; DTT, dithiothreitol. To lighten the notation and to avoid confusing superscripts, we refer to the standard molar changes in free energy, enthalpy, entropy, and volume, respectively, by $\&G$, $\&H$, $\&S$, and $\&V$.

0006-2960/89/0428-2144$01.50/0

pressure yields a straight line. Its slope gives $\&V$, the standard change in volume upon association, and the intercept the dissociation constant at atmospheric pressure. We have generally obtained these parameters by employing the range of degree of dissociation between 0.1 and 0.9. $\&V$ may also be obtained directly from the pressure span that covers this range of dissociations, dp, by means of a simple relation (Weber, 1986), which for tetramers is

$$\&V = 5RT \ln 9/\mathrm{d}p \quad (5)$$

when dp is given in kbar and $\&V$ in mL mol^{-1}. For 0 °C eq 5 gives $\&V = 249.5/\mathrm{d}p$. Equations 1–5 are simple consequences of the constancy of the chemical potentials of tetramer and monomer and are therefore independent of the intermediate equilibrium steps, involving perhaps trimers or dimers, in the path of dissociation of the tetramer into monomers. In the actual equilibria induced by pressure, or increasing dilution, these intermediate forms may be present in appreciable amounts, and we need to know how their presence affects the conclusions that one may reach in applying the thermodynamic formulation that includes only tetramer and monomers. To this purpose, we consider the likely situation in which the equilibria involve stepwise dissociation of the tetramer into dimers and of these into monomers. Besides serving the present purpose, such treatment is indispensable in interpreting the kinetics of reassociation into tetramers upon removal of the pressure, because a fourth-order process of monomer association involving no appreciable amounts of intermediates can be safely excluded.

Tetramer–Monomer Equilibrium with the Dimer as Intermediate. This involves the reactions T ↔ 2D and D ↔ 2M with the respective dissociation constants

$$K_{TD} = 4a^2C_{TD}/(1 - a) \qquad K_{DM} = 4b^2C_{DM}/(1 - b) \quad (6)$$

Here K_{TD} and K_{DM} are the dissociation constants of the tetramers into dimers and the dimers into monomers, respectively, and a and b the corresponding degrees of dissociation. C_{TD} and C_{DM} are the concentrations, in tetramers and dimers, respectively, involved in the two equilibria in eq 6. The equilibrium condition is that the concentration of dimers given by the two equations should be equal:

$$2aC_{TD} = (1 - b)C_{DM} \quad (7)$$

We computed the equilibrium condition by an iteration method in which tetramers, dimers, and monomers (T, D, and M, respectively) are expressed as fractions of the total protein concentration as tetramer, C given in units of K_{TD}. The iteration starts with initial values T_1, D_1, and M_1:

$$C_{TD} = (T_1 + D_1)C \quad C_{DM} = 2(D'_1 + M_1)/(K_{TD}/K_{DM}) \quad (8)$$

$D'_1 = 2aC_{TD}$ is the value of D obtained by solution of the first equation in eq 6 after introduction of the initial values of T and D, usually 1 and 0, respectively. b is obtained by solution of the second of equations (eq 6) with C_{DM} given by eq 8. $D_2 = (1 - b)C_{DM}(K_{TD}/K_{DM})$ and $T_2 = (1 - a)C_{TD}$ are reintroduced into the first equation (eq 6), and the process is continued until eq 7 is satisfied within a preassigned small error. The procedure may be checked by noticing that if $C/K_{TD} = 1.75$ and $K_{TD}/K_{DM} = 1$, one should obtain $T = 1/1.75$, $D = 0.5T$, and $M = 0.25T$. The described procedure involves then two parameters: C/K_{TD} and K_{TD}/K_{DM}. If the effects of pressure are sought, there are two additional ones, the standard volume changes for the two steps, $\&V_{TD}$ and $\&V_{DM}$. These determine the changes in the previous two parameters with pressure through the relations

$$K_{TD}(p) = K_{TD}(1) \exp(p\&V_{TD}/RT)$$
$$K_{DM}(p) = K_{DM}(1) \exp(p\&V_{DM}/RT) \quad (9)$$

where (p) and (1) indicate values at pressure p and atmospheric pressure, respectively. By systematic variation of these four parameters over the range that we expect to be significant for our case, we can estimate the merits of eq 4 when this is applied to analyze a process that occurs through the stepwise dissociation or reassociation of the tetramer. The results quoted in Table I refer to three possible cases: $\&V_{TD} = 3\&V_{DM}$, $\&V_{TD} = \&V_{DM}$, and $\&V_{TD} = \&V_{DM}/3$. The values of the table indicate that application of eq 4 yields an *average* standard volume change which is virtually the sum of $\&V_{TD}$ and $\&V_{DM}$ if $\&V_{TD}$ is larger than or equal to $\&V_{DM}$. If $\&V_{TD} = \&V_{DM}$, the logarithmic plots are virtually linear, but a departure from linearity becomes evident when $\&V_{TD}$ is conspicuously larger than $\&V_{DM}$. In the opposite case, when $\&V_{TD} < \&V_{DM}$, the linear relation of p and ln K_P is conserved, but the calculated volume may exceed considerably (by as much as 50%) $\&V_{TD} + \&V_{DM}$. Thus if a plot according to eq 4 is linear, we can exclude the case $\&V_{TD} > \&V_{DM}$, but the volume calculated by eq 4 must be treated as an apparent volume that may be fractionally larger than the sum of the volumes changes in the two successive association reactions.

Materials and Methods

The methods of determination of the degree of dissociation by measurements of the displacement of the center of mass of tryptophan emission as a function of pressure or by the change in polarization of the protein appropriately labeled with a dansyl fluorochrome are described elsewhere (Paladini & Weber, 1981; Silva et al., 1986; Ruan & Weber, 1988).

Glyceraldehydephosphate dehydrogenase from yeast was obtained from Boehringer Corp. Enzyme solutions were dialyzed for 3 h against three succesive lots of 1-L volume of standard buffer (0.05 M, pH 7.5, Tris buffer, 0.001 M in EDTA and in DTT) to remove traces of ammonium sulfate. Particulate matter of diameter greater than 2 μm was removed by a syringe filter. Protein concentration was determined by absorbance at 280 nm, employing a standard optical density for 1-cm depth of 0.1% solution of 0.89 (Kirschner et al., 1968). ADP, ATP, NAD, and c-AMP were from Sigma, 2-(dimethylamino)-5-naphthalenesulfonyl chloride was from Molecular Probes, and D_2O was from Aldrich Chemical Co. All other reagents were of analytical grade. Water was distilled and purified by passage through a Millipore system to a resistance of 18 MΩ. Enzyme activity was assayed at 25 °C and pH 7.5 by measuring the increase in absorption at 340 nm caused by the reduction of NAD (Allison & Kaplan, 1964). The pressure devices and the method of measurement of polarization under pressure (L format) are described by Paladini and Weber (1981a). Fluorescence spectra were determined as described by Royer (1985). Absorption measurements were done with an Acta MIV Beckman spectrophotometer.

Results and Their Interpretation

Curves 1 and 2 of Figure 1 show plots of the center of mass of the intrinsic fluorescence of 45 nM and 450 nM solutions of GAPDH against pressure at 0 °C. Plateau values are reached at 2.2 and 2.6 kbar, respectively, with very similar spectral red shifts of ca. 670 cm^{-1}. The spectra at 1 bar and 2.4 kbar are shown in the inset. Fluorescence red shifts on dissociation are observed in enolase (Paladini & Weber, 1982), B_2 tryptophan synthase (Silva et al., 1986), and hexokinase (Ruan & Weber, 1988). They indicate a considerable increase

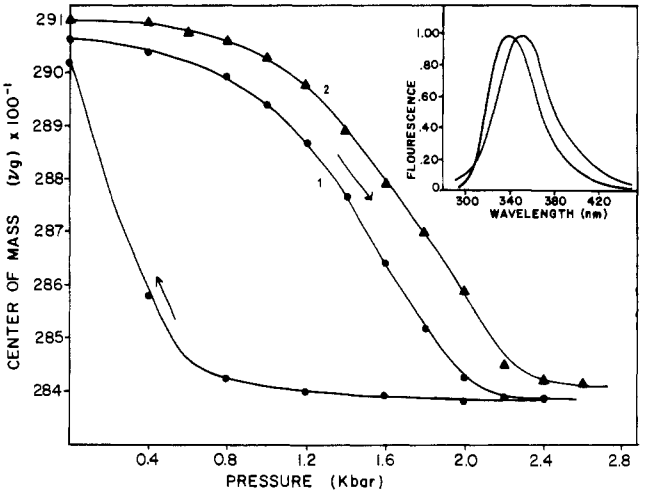

FIGURE 1: Center of mass, $\langle \nu_G \rangle$, of the intrinsic fluorescence of GAPDH excited at 280 nm as a function of applied pressure, for two protein concentrations. Curve 1: Pressure increase and decrease for 4.5×10^{-8} M GAPDH. Curve 2: Increasing pressure only for 4.5×10^{-7} M GAPDH. Inset: fluorescence emission spectra of solution 1 at 1 bar and 2.4 kbar.

Table I: Apparent Molar Changes in Association Volume, $\langle \& V \rangle$, Derived by Use of Equation 4 When the Association Steps Monomer → Dimer and Dimer → Tetramer Have Volume Changes $\& V_{TD}$ and $\& V_{DM}$[a]

C/K_{TD}	K_{TD}/K_{DM}	$\& V_{TD}$	$\& V_{DM}$	$\langle \& V \rangle$	$p_{1/2}$	slope
100	0.01	100	100	270	0.600	1
1 000	0.01	100	100	270	1.156	1
100	0.01	150	50	217	0.656	2
1 000	0.01	150	50	199	1.204	2
1 000	0.001	150	50	226	0.905	2
10 000	0.001	150	50	216	1.505	2
100	0.01	50	100	326	0.511	1
1 000	0.01	50	100	337	1.080	1

[a] Slopes refer to the number of distinct slopes that may be visually appreciated in the plots according to eq 4. $\langle \& V \rangle$ is the association volume from d ln K/dp averaged along the compression curve between the values of $a = 0.1$ and $a = 0.9$. Two concentrations differing by a factor of 10 are presented to demonstrate that in all the cases the displacement of $p_{1/2}$, the calculated pressure of half-dissociation, is of the magnitude predicted by eq 5.

in polarity of the tryptophan environment. A decrease in fluorescence efficiency is observed in all these cases, and in GAPDH it amounts to a loss of 50% at the pressures of complete dissociation. Plots according to eq 4 yield $\& V = 201$ and 199 mL mol^{-1} for the two protein concentrations, and eq 5 yields 200 and 195 mL mol^{-1}. The coincidence of the values obtained from eq 4 and 5 is proof of the good linearity of the plot according to eq 4. When two protein tetramer concentrations C_1 and C_2 are employed, the difference in pressure dp at which the same degree of dissociation is observed [Weber (1986), eq 11 and 13] is

$$\mathrm{d}p = RT \ln (C_2/C_1)^3/\& \mathrm{d}V \qquad (10)$$

When $\& V = 200$ mL and $C_2/C_1 = 10$ are introduced in eq 10, we obtain dp = 784 bar. The pressures $p_{1/2}$ at which $a = 1/2$ at the two concentrations are 1.25 and 1.41 kbar, or $\mathrm{d}p_{1/2} = 160$ bar, nearly one-fifth of the expected value. By reference to Table I we note that the existence of different volume changes in the dissociation involving the dimer as intermediate does not alter conspicuously the shift of the compression curve with protein concentration predicted by eq 10.

Independent proof of GAPDH dissociation is obtained by measurements of the pressure dependence of the fluorescence

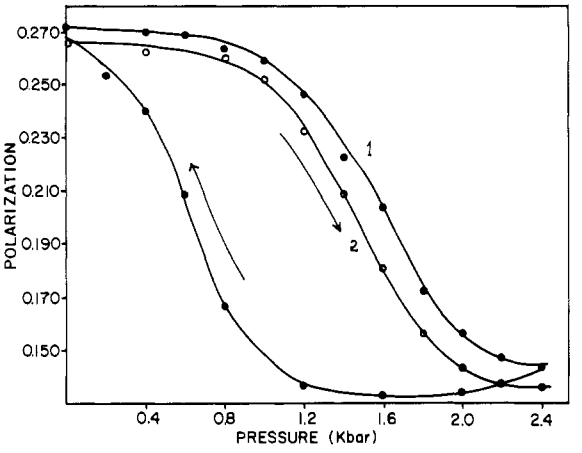

FIGURE 2: Polarization of the fluorescence of 2,5-DNS conjugate of GAPDH: curve 1, 10^{-7} M protein; curve 2, 2×10^{-8} M. Excitation at 380 nm; emission detected through 3-73 Corning filter and 3-mm layer of 2 M $NaNO_3$ solution.

polarization of 2,5-DNS conjugates of the protein. Figure 2 gives the plots of polarization of DNS fluorescence against the applied pressure for 20 and 100 nM solutions of GAPDH, respectively. For polarizations p_1 and p_2 and equal fluorescence lifetimes and limiting polarizations p_0, the Perrin equation gives the ratio r of the corresponding rotational relaxation times:

$$r = (1/p_1 - 1/p_0)/(1/p_2 - 1/p_0) \qquad (11)$$

With $p_1 = 0.27$, $p_2 = 0.140$, and $p_0 = 0.408$, eq 11 gives $r = 0.27$ clearly consistent with the dissociation of the tetramer into monomers but much too small for dissociation of the tetramer into dimers. For the observed fluorescence lifetime of 25 ns the values of the rotational relaxation times of the aggregate and dissociated particle are respectively 126 and 33 ns, in reasonable agreement with their respective sizes. Plots according to eq 4 respectively give $\& V = 231$ and 239 mL mol^{-1} for the two concentrations employed, while the corresponding values from eq 5 are 223 and 234 mL mol^{-1}. We note that in GAPDH, like in enolase, the values of $\& V$ obtained by the methods of spectral shift and fluorescence polarization are in much better agreement that in the cases of lactate dehydrogenase (King & Weber, 1986) and hexokinase (Ruan & Weber, 1988). The change in midpoint pressure with concentration, $\mathrm{d}p_{1/2} = 140$ bar, is less than one-third of the expected value (477 bar) so that the large discrepancy between the observed concentration displacement of the plots and that predicted by eq 4 is made quite evident by the two spectroscopic methods employed. The values of $\& V$ calculated according to eq 10 are in the range of 800–900 mL/mol; therefore, several times larger than those observed for dimer dissociation. Because of the considerable increase in the area of subunit contacts of tetramers in comparison with that of dimers, a figure of this magnitude does not seem unreasonable. We are thus inclined to believe that the shift of the compression curves on changing the concentration yields the more reliable value for $\& V$. As discussed in Appendix B the anomalously small values computed from the pressure span of the compression curves can result from a broad distribution of free energies of association in the tetramer population. We have been unable to find any assumption, other than the heterogeneity of the native tetramer population, that predicts displacements of the compression curves with concentration significantly different from those demanded by eq 10.

The values of $C_{1/2}$ at atmospheric pressure obtained by the two spectroscopic methods employed are somewhat different: 0.94 nM by spectral shift and 0.15 nM by DNS polarization.

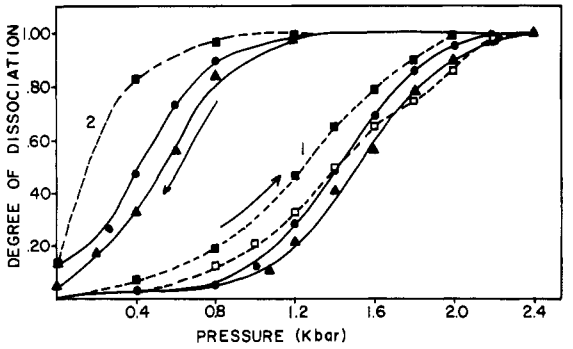

FIGURE 3: Plot of the data of curves 1 of Figures 1 (dashed line) and 2 (solid line) as degrees of dissociation versus pressure.

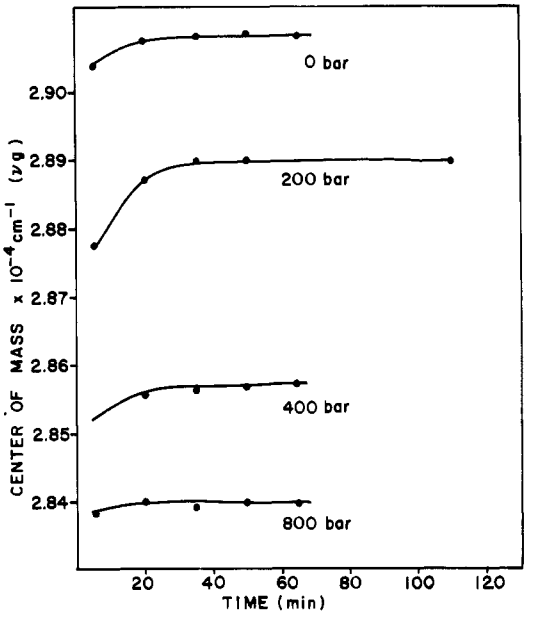

FIGURE 4: Kinetics of equilibration of GAPDH on partial decompression as followed through the center of mass of the emission. Plot of the center of mass versus time for 2 × 10^{-8} M GAPDH.

Such a difference contrasts with the very good agreement observed in dimers (Silva et al., 1986; Ruan & Weber, 1988), but it is one to be expected if there is a broad distribution of free energies of association in the native tetramer population. As the fluorescence polarization of the dansyl conjugates is likely to be less influenced than the tryptophan fluorescence by differences in free energy of association, we consider $C_{1/2}$ = 0.15 nM to be closer to the actual mean GAPDH value.

Hysteresis Phenomena. Figure 3 shows plots of the degrees of dissociation calculated from data obtained by the two spectroscopic methods during both compression and decompression. As already evident in Figures 1 and 2 a remarkably large hysteresis effect is observed on decompression. When the pressure was reduced from that of complete dissociation (2.4 kbar) to 0.8 kbar, 5% of the monomer reassociated, and no further change was recorded upon waiting for times 10-fold longer than those required to reach apparent equilibrium; 50% reassociation required reduction of the pressure to 0.16 kbar. The difference between this value and that obtained in the original compression, 1.25 kbar, is 1090 bar. The values of degree of dissociation on decompression at 0 °C were extremely stable as shown by the kinetic observations of Figure 4. The nearly complete recovery of the initial center of spectral mass of the intrinsic protein fluorescence and of the initial dansyl fluorescence polarization indicates that virtually all the tetramers reassociated on decompression. The large difference in the properties of the recovered tetramer, T*, and

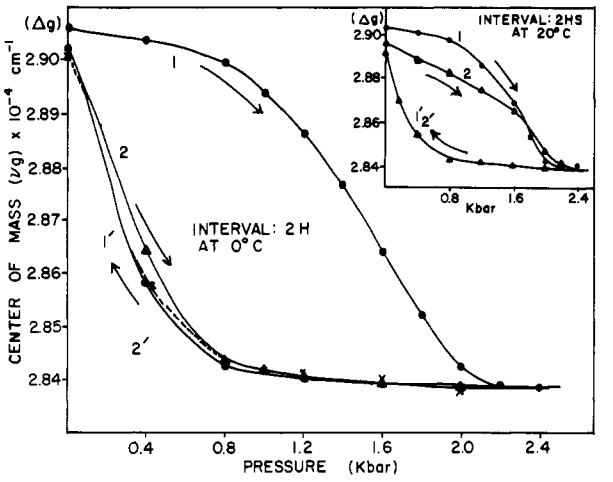

FIGURE 5: Change in the center of mass of the intrinsic emission of GAPDH, excited at 280 nm, as a function of pressure in two successive cycles of compression and decompression at 0 °C. First cycle, curves 1 and 1′; second cycle, curves 2 and 2′. Inset: A duplicate experiment except for a 2-h incubation at 20 °C between the two cycles.

the original tetramer, T, are best displayed when a second cycle of compression and decompression is carried out after a 2-h wait at 0 °C and atmospheric pressure (Figure 5). The new compression and decompression branches neatly overlap each other and the decompression branch of the first cycle, indicating that T* is a stable form that has reached limiting differences with the original tetramer, T. Free energies and standard volume changes of association are very different in both species: $C^*_{1/2}$ = 69 nM while $C_{1/2}$ = 0.15 nM, corresponding to a loss in free energy of association of 3.23 kcal mol^{-1}; $\&V^*$ equals 400 mL mol^{-1} and is twice as large as $\&V$ calculated from the pressure span but half of the value calculated from the displacement of the compression curves with concentration. We note that in the case of hexokinase, in which $\&V(p) = \&V(c)$, the drifted dimer had also a $\&V$ value approximately half of the native species. At 0 °C, the pressure equilibria in the second cycle involve exclusively the forms T* and M* while the equilibria during the original compression are evidently more complex, involving the various forms that result from the conformational drift. The tetramer recovered after decompression did not exhibit any enzymic activity but slowly recovered it when brought to room temperature, a phenomenon already observed by King and Weber (1986a) in the lactate dehydrogenases. Total enzymic inactivation of GAPDH may be obtained by complete dissociation by pressure followed by decompression or by lengthier incubation under a lower pressure at 0 °C. In either case recovery of activity required incubation at room temperature. The regain of the initial values of $C_{1/2}$ and $\&V$ at room temperature is demonstrated by repeating a second cycle of compression and decompression at 0 °C, but after a delay of 2 h at 20 °C. As the inset of Figure 5 shows, under these conditions there is almost complete recovery of the original values of $C_{1/2}$ and $\&V$, as well as transformation into the drifted form after the second cycle. The conformational drift, the almost complete recovery from it after a period at room temperature, and its recurrence during a second cycle of compression are virtually carbon copies of phenomena observed already in lactate dehydrogenase (King & Weber 1986a). All these observations conform to the energetic scheme proposed by Figure 1 of King and Weber (1986b) for the cold inactivation and room temperature reactivation of lactate dehydrogenase.

Numerical Simulation of the Hysteresis Phenomena. In a previous paper (Weber, 1986) we proposed a model that

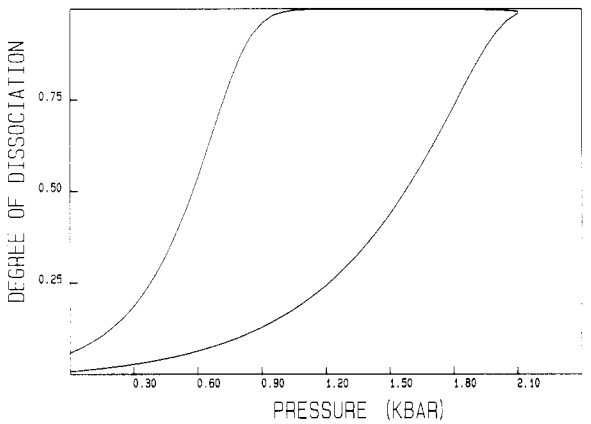

FIGURE 6: Simulation of the hysteresis on decompression as described in Appendix A. The parameters used in the simulation shown in the figure were $C^*_{1/2}/C_{1/2} = 18$, $C/C^*_{1/2} = 400$, & $V = 200$ mL mol^{-1}, & $V^* = 400$ mL mol^{-1}, $S = 0.02$, and $R = 0.0001$; 50 iterations. The difference in $p_{1/2}$ between ascending and descending pressures is 1008 bar.

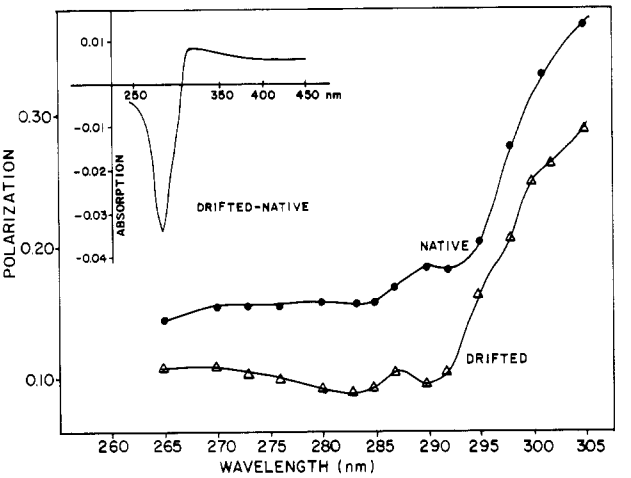

FIGURE 7: Excitation polarization spectra of the intrinsic fluorescence of native and drifted 4.5×10^{-8} M GAPDH. Emission detected through Corning filter 0–54. Inset: The differential absorbancy (drifted − native) of 4.5×10^{-7} M solutions. All observations at 0 °C.

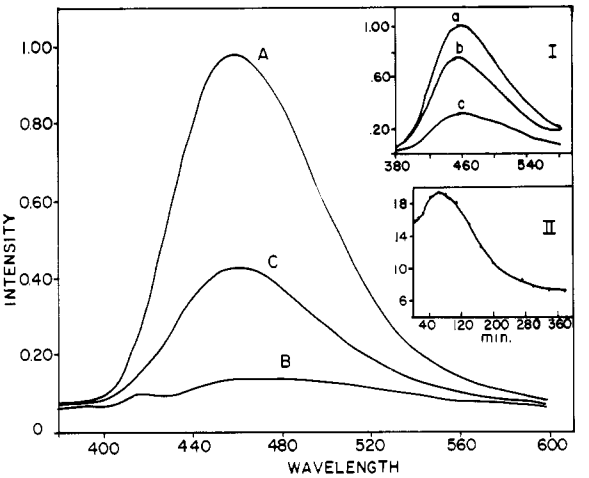

FIGURE 8: Spectra of complexes of GAPDH (4.5×10^{-8} M) with ANS (5×10^{-5} M) and NADH (1×10^{-4} M): (A) ANS drifted tetramer; (B) ANS native tetramer; (C) ANS temperature-reactivated tetramer. (Inset I) Spectra of protein–NADH: (a) with drifted GPDH; (c) with native GAPDH; (b) with reactivated GAPDH. (Inset II) Time course of the fluorescence intensity changes of drifted GAPDH–ANS during 20 °C reactivation.

permits the quantitative description of the phenomena of conformational drift and hysteresis. The application of this model to GAPDH is particularly pertinent as this protein presents the most extreme case of hysteresis that we have sofar observed. We recall that the model supposes the existence of at least two forms of tetramers (T and T*): the former includes only subunits (M) in the "native" state; the other is made up of conformationally modified, "drifted", monomers (M*). The association–dissociation equilibria of both types of aggregates are supposed to proceed rapidly in comparison with the rates of the first-order reactions that convert M into M* or T* into T. We neglect the corresponding opposing reactions, M* → M and T → T*. There is in fact no experimental evidence that these reactions take place at all. The violation of reciprocity thus implied is discussed in detail elsewhere (Xu & Weber, 1982; Weber, 1986, 1987). Here we are only concerned with providing an appropriate numerical simulation of the phenomena observed upon successive compression and decompression of the protein solutions. A description of the method employed is given in Appendix A. We stress that the proposed model is far from giving a complete or accurate description of all the aspects involved. Its main shortcoming derives from the treatment of a many-steps process as an equilibrium between two unique molecular forms. Figure 6 shows a compression–decompresson profile that closely follows that observed in the experiments with GAPDH. The application of this simulation procedure to kexokinase is given elsewhere (Ruan & Weber, 1988).

Physical Differences between Native and Drifted Tetramers. The preceding observations show that complete dissociation by application of pressure and subsequent decompression at 0 °C transform completely T into T* and that this form is stable so long as the low temperature is maintained. It thus makes it possible to reveal physical differences of T and T* by a comparison, at 0 °C, of the properties of identical solutions of protein, one of which was previously subjected to a cycle of compression and decompression. The conformationally drifted form that we studied was prepared by incubating a 45 nM solution of GAPDH in standard buffer at 0 °C at a pressure of 2.4 kbar for 1 h, or a micromolar solution for 3 h, and then gently releasing the pressure.

Spectral Differences. Figure 7 shows the excitation polarization spectra of the fluorescence of native and drifted protein. There is a significant decrease in polarization throughout the excitation range indicating an increase in the local mobility of the tryptophan in the drifted form. Additionally, the secondary maximum of polarization at 290 nm (Weber, 1960; Valeur & Weber, 1976) is blue-shifted in the drifted form indicating an underlying relative shift of the L_b transition in the same direction. This latter conclusion can also be reached by examination of the differential absorption of the samples shown in the same figure: a minimum is observed at 280 nm. The fluorescence lifetimes showed only a small difference: 4.24 ns for T* and 4.68 ns for T. The relative fluorescence yields of native tetramer, drifted monomer, and drifted tetramer were respectively 1:0.48:0.63, suggesting the persistence of the structure of the drifted monomer within the corresponding tetramer.

Binding Differences. 1-Anilino-8-naphthalenesulfonate is known to bind with high affinity to several dehydrogenases occupying the binding site for NAD, as proven by competition experiments (Ellenrieder et al., 1972). Figure 8 shows that drifted GAPDH binds ANS with a 24-fold increase in the yield of fluorescence of the free ligand and a spectral blue shift of 13 nm when compared with the protein before compression. Smaller but evident differences in the fluorescence yield and

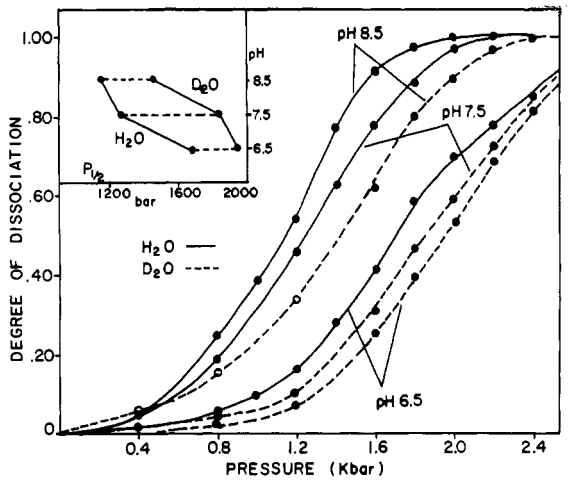

FIGURE 9: Plots of degree of dissociation of GAPDH, determined by the center of mass of the emission at several pH values, against pressure: 4.5×10^{-8} M protein concentration in standard buffer at 0 °C. (Inset) Plot of $p_{1/2}$ to show the differences in the effects of D_2O and H_2O with pH.

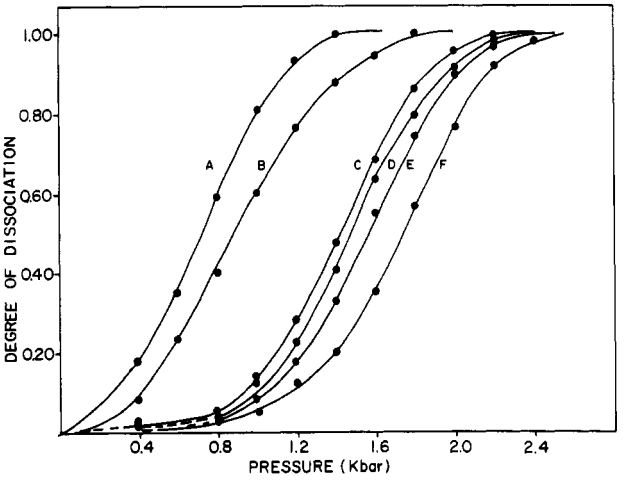

FIGURE 10: Plots of degree of dissociation, from fluorescence polarization of 2×10^{-8} M dansyl conjugates of GAPDH, at 0 °C in the presence of ligands: (A) ATP; (B) ADP; (C) none; (D) D-glyceraldehyde 3-phosphate; (E) c-AMP; (F) NAD. All ligands at 1×10^{-3} M.

Table II: Pressure Dissociation of GAPDH in H_2O and D_2O at 0 °C

pH	solvent	$\&V$ (mL mol^{-1})	$C_{1/2}$ (nM)	$\&G$ (kcal)
6.5	H_2O	158	0.69	−32.3
7.5	H_2O	201	0.95	−31.9
8.5	H_2O	212	1.25	−31.4
6.5	D_2O	182	0.23	−34.3
7.5	D_2O	174	0.71	−32.4
8.5	D_2O	171	1.15	−31.6

Table III: Effect of Various Ligands on the Pressure Dissociation of GAPDH at 0 °C

ligand	$\&V$ (mL mol^{-1})	$C_{1/2}$ (nM)	$\&G$ (kcal)
(A) Measured by Fluorescence Polarization of Dansyl-GAPDH			
none	230	0.15	−34.9
ATP	237	1.51	−31.2
ADP	178	1.87	−30.8
c-AMP	241	0.067	−36.2
NAD	241	0.037	−37.2
GAP[a]	224	0.13	−35.1
(B) Measured by Spectral Shift of the GAPDH Fluorescence			
none	201	0.95	−31.9
GAP	200	0.94	−32.0
glycerol (10%)	143	0.91	−32.0
glycerol (25%)	86	1.18	−31.5
S-(carboxymethyl)cysteine	180	1.39	−31.3

[a] GAP: glyceraldehyde 3-phosphate.

spectrum of bound NADH were also observed (inset of Figure 8). These differences in the complexes of T and T* with ANS or NADH indicate appreciable modifications at the active site, which one would expect to correlate with the inactivation of the enzyme.

Effects of pH and of D_2O. Figure 9 shows the dissociation profiles of GAPDH at three pH values in both H_2O and D_2O. Calculated $C_{1/2}$ and $\&V$ are displayed in Table II. A decrease of 50 mL mol^{-1} in $\&V$ was observed at pH 6.5, just like in the case of hexokinase (Ruan & Weber, 1988), indicating here also the importance of a charged group at the subunit interface with a pK close to 7. Maximum stability in both water and deuterium oxide was found at pH 6.5. In water at pH 7.5 the association was less stable than that at pH 6.5 by 0.5 kcal and by 1.0 kcal at pH 8.5. The curves for D_2O are systematically displaced to higher pressures with respect to the values in H_2O, and the difference $H_2O - D_2O$ was significantly larger (1.9 kcal) at pH 7.5 than at pH 6.5 (0.5 kcal) or at pH 8.5 (0.3 kcal). The dependence of the differences in $\&V$ and $C_{1/2}$ in the two solvents upon pH indicates that they arise from charge properties rather than from solvent effects upon nonpolar interactions. Addition of glycerol had an evident stabilizing effect: 10% glycerol resulted in a decrease of $\&V$ of 58 mL, and at 25% glycerol the decrease was 115 mL, indicating that the pressure stabilization resulted from decreased $\&V$. The explanation of this volume effect may be that replacement of the much smaller water molecules by those of glycerol results in less complete disappearance of any packing defects at the intersubunit interfaces upon dissociation.

Effects of Substrates and Modifiers. These are shown in Figure 10, and the derived parameters are gathered in Table III. ADP and ATP, two compounds that are known allosteric inhibitors of the enzyme (Stacel & Deal, 1968), had an obviously destabilizing effect showed by $p_{1/2}$ shifts of −720 and −526 bar, respectively. The standard free energies of association were increased by 3.7 and 4.1 kcal, respectively. Although the values of $C_{1/2}$ were thus quite close, ADP decreased $\&V$ by 45 mL mol^{-1} while ATP had no obvious effect upon the volume change. The effect of cAMP was opposite, and considerably smaller than those of ADP and ATP: it changed the free energy of association by −1.3 kcal mol^{-1} and shifted $p_{1/2}$ by +130 bar. D-Glyceraldehyde 3-phosphate did not seriously affect the association free energy, but the red shift in the center of mass of tryptophan fluorescence upon dissociation was reduced from 670 to 390 cm^{-1}, indicating that the substrate had a specific effect upon the fluorescence spectrum of the monomers and no appreciable effect upon that of the tetramer or indicating that glyceraldehyde phosphate limited the dissociation, e.g., to dimers. However, this latter explanation was excluded because the values of fluorescence polarization of the dansyl conjugates reached at high pressure were no different in the absence and presence of this ligand. NAD decreased the standard free energy of association by −2.3 kcal and shifted $p_{1/2}$ to higher pressure by 320 bar.

Temperature Stability. Pressure dissociation curves of GAPDH at various temperatures in the interval of −5 to 30 °C are presented in Figure 11. We note that because of the depression of the freezing point of water with pressure, it is possible to explore the effect of pressure at temperatures below 0 °C. The curves in Figure 11 shift to higher pressures as the temperature is raised, indicating an increase in stability with temperature. The dissociation constants *increase slowly with temperature*, but the standard free energies of association

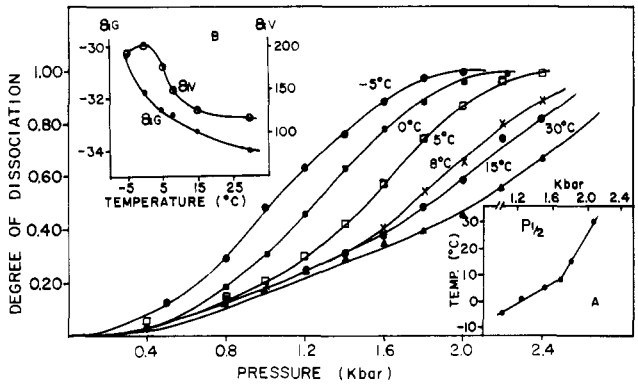

FIGURE 11: Plots of degree of dissociation of GAPDH versus pressure at different temperatures derived from measurements of changes in center of mass of intrinsic fluorescence of 4.5×10^{-8} M solutions at 0 °C. (Inset A) Plot of $p_{1/2}$ against temperature. (Inset B) Plots of $\&G$ and $\&V$ against temperature.

Table IV: Pressure Dissociation of GAPDH at Several Temperatures

temp (°C)	$C_{1/2} \times 10^{10}$	$\&G$ (kcal mol^{-1})
-5	17.4	-30.3
0	9.5	-31.9
5	9.8	-32.4
8	11.0	-32.6
15	11.9	-33.3
25	18.2	-33.7
30	20.1	-34.1

(Table IV) increase in absolute value with the temperature because the RT factor in the equation $\&G = RT \ln K$ more than compensates for the apparent increase in K. If the free energy of association at lowest temperature, T, is $\&G_L$ and at highest temperature, $T + dT$, it equals $\&G_L + dG$, then the estimated enthalpy change is

$$\&H = \&G_L - dG(T/dT) \qquad (12)$$

With the values of $\&G$ at 0 and 30 °C of Table IV we thus estimate $\&H$ to be −12 kcal mol^{-1}. By eq 12 it is evident that the enthalpy of association in hexokinase (Ruan & Weber, 1988) is large and positive, indicating that the enthalpy of hydration of the interfaces must be appreciably larger in yeast hexokinase than in GAPDH. $\&V$ steadily decreased with temperature (upper left inset of Figure 11), and the decreases in $\&V$ and $\&G$ worked together to give a rise of 1 kbar in $p_{1/2}$ when the temperature rose from −5 to 30 °C (lower right inset). It is not clear what physical significance ought to be attributed to the value of $C_{1/2}$ obtained by extrapolation to atmospheric pressure at −5 °C, as it refers to a condition that is not physically realizable; it is noticeable from the table that there is an evident discontinuity between the value of $C_{1/2}$ at −5 °C and the values obtained at temperatures above 0 °C. For this reason we did not include it in the van't Hoff plot from which the enthalpy change upon association, $\&H$, was calculated. This plot yields $\&H = -14.10$ kcal mol^{-1} so that at 25 °C, for which $\&G = -33.4$, $\&S = T\&S = +19.3$ kcal mol^{-1}. The increase in entropy upon association is all important in the stability of the GAPDH tetramer; if the entropy did not increase upon monomer association, the concentration for half-dissociation of the tetramer would be 1×10^{-4}, and the protein would be in the monomer form at all practical concentrations. We note that the increase in entropy upon association seen in various oligomeric aggregates is of uncertain origin, as we discussed in relation to the hexokinase data (Ruan & Weber, 1988).

Kinetics of Dissociation and Association. Like in the case of other aggregates, dissociation proceeded slowly upon rapidly raising the pressure to 2.5 kbar. Figure 12 shows that the half-time for dissociation at 0 °C was about 15 min, corresponding roughly to a rate constant for dissociation of 1×10^{-3} s^{-1}. This time practically equals the rate of dissociation of the tetramer into dimers if the rates of dissociation are proportional to the corresponding dissociation constants. On this same premise the time course of the reassociation on decompression is largely determined by the rate of dissociation of the dimer into monomers, which is not directly accessible to measurement. The rapid recovery of the spectral properties on decompression indicates that, within the time resolution of our measurements, the rate of reassociation is not greatly affected by the conformational drift. The recovery of the enzyme activity at 20 °C (Figure 12) is evidently much slower than the reassociation, and both rate and final value of the recovered activity depend upon the time spent under a fully dissociating pressure. These phenomena have already been observed in the lactate dehydrogenases (Mueller et al., 1981; King & Weber, 1986a) and in the apoprotein of B_2 tryptophan synthase (Silva et al., 1986).

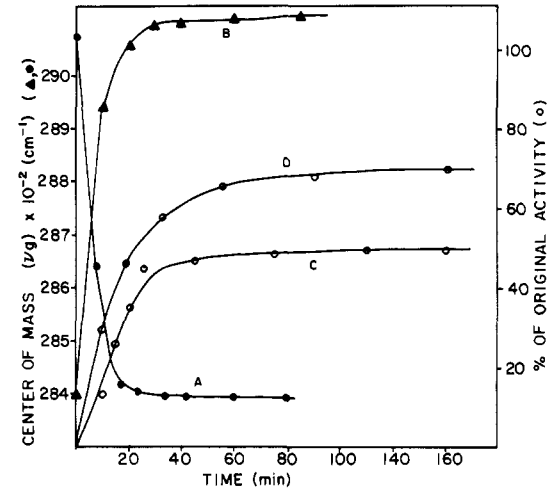

FIGURE 12: Time course of the dissociation after a rise in pressure from atmospheric to 2.4 kbar (A) and following rapid decompression of the same solution (B) at 0 °C. Curve D gives the recovery of enzyme activity at 20 °C after compression to 2.4 kbar for 30 min followed by rapid decompression. (C) Activity when the compression was held for 90 min. All observations at 0 °C, with protein concentrations of 4.5×10^{-8} M.

Conclusions

The observations presented in this paper and in several previous ones (Paladini & Weber, 1981; King & Weber, 1986a,b; Silva et al., 1986; Ruan & Weber, 1988) permit us to draw some general conclusions about the stability and dynamics of oligomeric proteins, particularly dimers and tetramers. In dimers the situation appears simpler: After dissociation by compression followed by decompression, the dimers reassociate into a species with diminished affinity and enzyme activity but rapidly recover both, whether at room or cold-room temperatures. The values of $\&V$ from the change in dissociation with pressure are very similar to those derived by the shift in dissociating pressure with protein concentration, indicating that the dimer population is relatively homogeneous as regards both free energy and volume change of subunit association. In the three tetramers that we studied (porcine and bovine LDH and yeast GAPDH), the situation is more complex: the tetramers recovered after decompression have diminished free energy of association and greatly diminished enzyme activity like the dimers. When warmed to room temperature, they fully recover the initial values, but at low

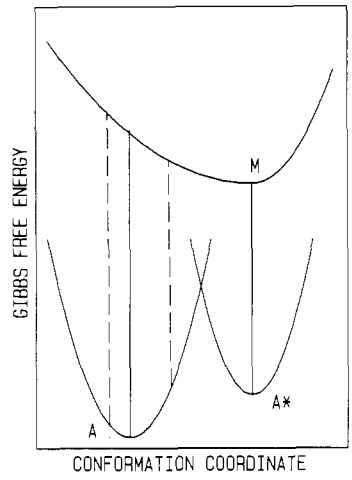

FIGURE 13: Free energy dependence upon the conformational coordinates of aggregate A and A* and monomer M. It differs from the scheme previously proposed by King and Weber (1986b) in that the monomer is assumed to have a single stable form and correspondingly the aggregate always forms a heterogeneous population.

temperature (0–5 °C) they retain, apparently indefinitely, the diminished activity and affinity that followed the dissociation. Native tetramers undergo progressive inactivation when kept in micromolar solution at *4* °C *and atmospheric pressure* for several weeks, and the cold-inactivated species shows similarity as regards diminished subunit affinity and other physical properties with the tetramers recovered after decompression. In all the tetramers studied it was observed that the values of ΔV calculated from the shift of the compression curves with protein concentration were about four times larger than those derived from the change in dissociation with pressure at any one concentration. This discrepancy reveals the existence of a considerably heterogeneity of free energies of association: The members of the tetramer population must differ from each other in many small conformational details that result from the different ways of interaction of the subunits. The existence of these differences seems inevitable if one accepts that the free monomers undergo conformational drift without losing the larger part of their affinity. Then, the continuous dissociation and association result in a population the characteristics of which depend upon the concentration and the temperature. To take these facts into account, we will slightly, but significantly, modify the energetic scheme of King and Weber (1986b). This is shown in Figure 13. It will be noticed that the dissociation of the dimer or tetramer does not result in a stable, or quasi-stable, monomer species as proposed in the original scheme. Instead, it corresponds to one of the many possible higher-energy forms of M, the stable minimum of which lies at a point of the conformational coordinate beyond the energy surface of the native tetramer population. The distribution of free energies of the native population results from the continuous dissociation of tetramers and limited conformational drift of the monomer followed by reassociation and to an unknown extent from fluctuations in tetramer conformation along the conformational coordinate that describes the differences in association free energy. As the M minimum lies beyond the energy surface of the tetramer, rapid reassociation of the stable monomers results in a form, the drifted tetramer or dimer A*, that can only revert slowly to the initial aggregate A. Although the nature of the process by which A* changes to A is still obscure, the strong dependence upon the temperature indicates that it requires a considerable energy, or more likely entropy, of activation. If the process of reactivation necessitates rearrangements of each subunit of the aggregate with respect to others with which it makes contact, it is then easy to see why dimers revert much more easily than tetramers to the original form, why the dimer population is much more homogeneous than that of tetramers, and why cold inactivation of dimers has not been reported.

In a paper of 1965 Monod et al. envisioned oligomeric proteins as existing in only two main conformations, T and R, determined by the disposition of the subunits in the aggregate. The equilibrium between these conformers was assumed to change by the binding of specific allosteric ligands, and this proposition has been used in the intervening years to explain changes in binding energies and enzyme activities of oligomeric proteins with limited success (Reinhart & Hartleip, 1986; Smith et al., 1988). The changes in sign and magnitude of the free energy of association of hexokinase (Ruan & Weber, 1988) and GAPDH caused by substrates and allosteric ligands are sufficient to indicate that oligomeric proteins exist in a variety of energetic states and that a simple bistable equilibrium is inapplicable. The heterogeneity of the free energy of association in the absence of ligands is equally conclusive.

Inactive drifted forms of tetramers can be obtained in the absence of the specific ligands, under conditions of incipient dissociation like cold temperature at atmospheric pressure. Such conditions, for example, high salt and low temperature, are often enough used in the crystallization of oligomeric proteins so that one may raise the question of the relation of the unique structures determined by X-ray analysis of these crystals to the evidently polymorphous population that is implied by the properties of the solutions. The recent observation of Liddington et al. (1988) that oxyhemoglobin can be crystallized in a form that shows large differences in the disposition of the helices and in the intersubunit salt bridges from the one originally described by Perutz and collaborators (1970) is in agreement with the general trend that we have observed in the properties of oligomeric proteins studied by hydrostatic pressure.

Appendix

(A) Simulation of the Hysteresis Effects on Decompression. The equilibria of the T and T* tetramers with the corresponding monomers M and M* at atmospheric pressure are described by equations equivalent to eq 3:

$$m^3 = a^4/(1-a) \qquad m^{*3} = a^{*4}/(1-a^*) \quad \text{(A1)}$$

where $m = (C_{1/2}/[C(1-f)])^3$, $m^* = [C_{1/2}/(Cf)]^3$, C is the total protein conentration as tetramer, and f is the fraction of the total protein in the drifted form. The values $m(p)$ and $m^*(p)$ at pressure p relate to the corresponding ones at atmospheric pressure through

$$m(p)^3 = m^3 \exp(p\mathrm{d}V^0/RT) \quad \text{(A2)}$$

$$m^*(p)^3 = m^{*3} \exp(p\mathrm{d}V^*/RT)$$

Exchanges between the two forms, native and drifted, are assumed to occur exclusively by the directional reactions M $\rightarrow$ M*, at rate S, and T* $\rightarrow$ T, at rate R. For convenience S and R will be assumed to be pressure independent. When the ratios $C_{1/2}/C$ and $C^*_{1/2}/C$, S and R, are given, a simple iteration procedure which imitates the actual kinetics of the system may be used to determine the values of a, a^*, and f in the system of eq A1. With any initial value of $f = f_0$ the equations above are solved (see below) to give a and a^*. The change in f resulting from transfer between the two systems is

$$\mathrm{d}f = -Sa(1-f)/4 + R(1-a^*)f \quad \text{(A3)}$$

The new value for f is $f_1 = f_0 + df$, and the iterative solution of eq A1 is continued until $df < e$, where e, a preestablished small value, is the acceptable defect in the equilibrium condition

$$Sa(1 - f)/4 = R(1 - a^*)f \quad \text{(A4)}$$

The corresponding average dissociation is

$$\langle a \rangle = a(1 - f) + a^*f \quad \text{(A5)}$$

The condition favorable to accumulation of the drifted form is $S \gg R$. For this condition, if the iteration process is continued for a number of cycles of order $1/R$, complete equilibration is reached, and the values of a as function of p obtained upon increase in pressure are the same as those obtained upon decompression following complete dissociation (Weber, 1986). When the number of iterations is limited to a value comprised between $1/S$ and $1/R$, the curves for compression and decompression are different and can reproduce remarkably well the experimentally observed hysteresis.

Numerical Solution of Equation A1. Obtaining the degree of dissociation as a function of concentration and pressure for an aggregate of n particles requires the solution of an equation of degree n of the form

$$a^n + Ba - B = 0 \quad \text{(A6)}$$

A numerical solution by the conventional methods is hampered by the existence of multiple roots, and to obtain the single positive root, we have used instead the following iterative procedure:

If $B < 1$, then $a_1(0)^n = B$, which makes $a_1(0) > a$:

$$a_2(0)^n = [1 - a_1(0)]B, \text{ which makes } a_2(0) < a \quad \text{(A7)}$$

If $B > 1$, then $a_1(0) = 1 - 1/B$, which makes $a_1(0) < a$:

$$a_2(0) = 1 - a_1^n(0)/B, \text{ which makes } a_2(0) > a \quad \text{(A8)}$$

The iteration proceeds by substituting $a_1(0)$ in the second equation of either pair above by $a_1(1) = [a_1(0) + a_2(0)]/2$, to yield $a_2(1)$, and continues until $a_2(N) - a_1(N)$ becomes smaller than the acceptable error in eq A6.

(B) Effects of a Heterogeneous Population upon the Compression Curves. We noted above that $\&V$, the standard volume change upon association, can be obtained from the change in degree of dissociation with pressure at constant protein concentration $[(da/dp)_C$, eq 5] or from the change in dissociation pressure with protein concentration for a fixed degree of dissociation $[(dp/dc)_a$, eq 10]. In three dimers studied, enolase (Paladini & Weber, 1982), B_2 tryptophan synthase (Silva et al., 1986), and hexokinase (Ruan & Weber, 1988), the values of $\&V$ given by the two methods, though not identical, were found to be in reasonable agreement (±20%). The situation is evidently different with tetramers: In the lactate dehydrogenases (King & Weber, 1986a), and as described above in the case of GAPDH, there is a big discrepancy in the values offered by the two methods. $\&V$ calculated by the change in $p_{1/2}$ with concentration is nearly four times larger than that calculated by the pressure span at either concentration. Numerical simulations carried out as described in Appendix A indicate that the conformational drift has no appreciable effect upon the displacement of the compression curves with concentration. The most reasonable explanation for the discrepancy between the values of standard volume change upon association determined by the two methods is that of heterogeneity of the population of protein molecules as regards the free energy of association or standard volume change, or both. The similarity of the effects owing to changes in these two quantities is appreciated on writing the dissociation free energy operative at pressure p in the form

$$\&G(p) = \&G_{atm} + p\&V \quad \text{(B1)}$$

Changes in $\&V$ and $\&G_{atm}$ in a population will result in almost parallel displacements of the plots of a vs pressure for the individual members of the population. In these circumstances the pressure span experimentally measured appears greatly increased and the calculated $\&V$ is correspondingly much smaller than the change in association volumes for the separate members of the population. Numerical simulation of the experimental results involves defining a population of free energies of association that can result in $\&V$, determined by the pressure span, close to 200 mL but with a shift of the pressure dissociation curves of only 150 bar when the concentration is changed by an order of magnitude. We find that a population of different association volumes cannot produce these large effects. On the other hand, Figure 14 shows that imitation of the effects observed in GAPDH is possible by postulating a very broad, skewed Gaussian distribution of free energies of association. The skewing is required in order to obtain an approximately linear plot of ln $K(p)$ against pressure. The standard deviations of the free energy of association, $-15RT$ and $+10RT$ respectively, correspond to 25 and 17% of the mean free energy of association, and their large value could be seen as casting doubt upon the validity of the proposed explanation. However, in spite of much searching we have been unable to find another assumption that quantitatively explains the observed effects. For a distribution of this type the values of ln $K(p)$ fall on a curve slightly concave toward the pressure axis as clearly shown in the figure by supperposition of the regression line that they determine. A very slight curvature of the same kind is actually shown by many experimental compression plots of GPDH. We believe that this observation is a strong independent argument in favor of a plurality of free energies of association of the intact tetramers, although the precision of our measurements is not yet good enough to permit its use to quantitatively define the tetramer population.

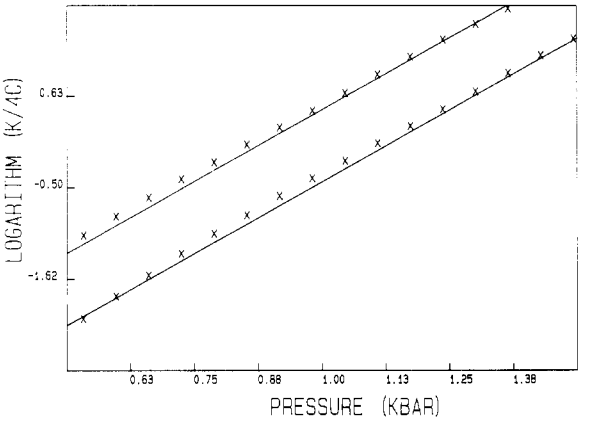

FIGURE 14: Plots according to eq 4, in decimal logarithms, for two protein concentrations that differ by a factor of 10. The free energy of association of the monomers into the tetramer protein is assumed to form a skewed Gaussian distribution (Appendix B) with a mean free energy of association of $57RT$ and standard deviations of $+15RT$ and $-10RT$, respectively. All fractions have $\&V = 800$ mL mol^{-1}. The plots show the calculated points (×) and the regression lines that they determine. Their slopes are characteristic of $\&V = 216$ mL mol^{-1}, but the shift with concentration gives $\&V = 800$ mL mol^{-1} when calculated by means of eq 10.

Registry No. GAPDH, 9001-50-7; ATP, 56-65-5; ADP, 58-64-0; c-AMP, 60-92-4; NAD, 53-84-9; GAP, 591-57-1; glycerol, 56-81-5;

S-(carboxymethyl)cysteine, 638-23-3.

REFERENCES

Allison, J., & Kaplan, N. O. (1964) *J. Biol. Chem. 239*, 2140–2152.

Ellenrieder, G. V., Kirschmer, K., & Schuster, I. (1972) *Eur. J. Biochem. 26*, 220–235.

King, L., & Weber, G. (1986a) *Biochemistry 25*, 3632–3637.

King, L., & Weber, G. (1986b) *Biochemistry 25*, 3637–3640.

Kirschner, K., & Voigt, B. (1968) *Hoppe Seyler's Z. Physiol. Chem. 349*, 632–644.

Liddington, R., Derewenda, Z., Dodson, G., & Harris, D. (1988) *Nature 331*, 725–728.

Monod, J., Wyman, J., & Changeux, J.-P. (1965) *J. Mol. Biol. 12*, 88–118.

Mueller, K., Luedemann, H.-D., & Jaenicke, R. (1981) *Biochemistry 20*, 5411–5416.

Paladini, A. A., & Weber, G. (1981a) *Rev. Sci. Instrum. 52*, 419–427.

Paladini, A. A., & Weber, G. (1981b) *Biochemistry 20*, 2587–2593.

Perutz, M. F. (1970) *Nature 228*, 726–739.

Reinhart, G., & Hartleip, S. (1986) *Biochemistry 26*, 7308–7313.

Royer, C. A. (1985) Ph.D. Thesis, University of Illinois.

Ruan, K., & Weber, G. (1988) *Biochemistry 27*, 3295–3301.

Silva, J. L., Miles, E. W., & Weber, G. (1986) *Biochemistry 25*, 5781–5786.

Smith, F., Gingrich, D., Hoffman, B. M., & Ackers, G. K. (1988) *Proc. Natl. Acad. Sci. U.S.A. 84*, 7089–7093.

Stacel, G. M., & Deal, W. C. (1968) *Biochem. Biophys. Res. Commun. 31*, 398–403.

Valeur, B., & Weber, G. (1977) *Photochem. Photobiol. 25*, 441–444.

Weber, G. (1986) *Biochemistry 25*, 3626–3631.

Weber, G. (1987) *NATO ASI Ser., Ser. C No. 197*, 401–420.

Xu, G.-J., & Weber, G. (1982) *Proc. Natl. Acad. Sci. U.S.A. 79*, 5268–5271.

EPR Characterization of the Iron–Sulfur-Containing NADH–Ubiquinone Oxidoreductase of the *Escherichia coli* Aerobic Respiratory Chain†

Steven W. Meinhardt,‡ Kazunobu Matsushita,§,‖ H. Ronald Kaback,§ and Tomoko Ohnishi*,‡

Department of Biochemistry and Biophysics, University of Pennsylvania, Philadelphia, Pennsylvania 19104, and Roche Institute of Molecular Biology, Roche Research Center, Nutley, New Jersey 07110

Received June 1, 1988; Revised Manuscript Received October 20, 1988

ABSTRACT: The energy coupled NADH–ubiquinone (Q) oxidoreductase segment of the respiratory chain of *Escherichia coli* GR19N has been studied by EPR spectroscopy. Previously Matsushita et al. [(1987) *Biochemistry 26*, 7732–7737] have demonstrated the presence of two distinct NADH–Q oxidoreductases in *E. coli* membrane particles and designated them NADH dh I and NADH dh II. Although both enzymes oxidize NADH, only NADH dh I is coupled to the formation of the H^+ electrochemical gradient. In addition to NADH, NADH dh I oxidizes nicotinamide hypoxanthine dinucleotide (deamino-NADH), while NADH dh II does not. In membrane particles we have detected EPR signals arising from four low-potential iron–sulfur clusters, one binuclear, one tetranuclear, and two fast spin relaxing $g_\perp = 1.94$ type clusters (whose cluster structure has not yet been assigned). The binuclear cluster, temporarily designated $[N\text{-}1]_E$, shows an EPR spectrum with $g_{x,y,z} = 1.92, 1.935, 2.03$ and the $E_{m7.4}$ value of −220 mV ($n = 1$). The tetranuclear cluster, $[N\text{-}2]_E$, elicits a spectrum with $g_{x,y,z} = 1.90, 1.91, 2.05$ and an $E_{m7.4}$ of −240 mV ($n = 1$). These two clusters have been shown to be part of the NADH dh I complex by stability and inhibitor studies. When stored at 4 °C, both clusters are extremely labile as is the deamino-NADH–Q oxidoreductase activity. Addition of deamino-NADH in the presence of piericidin A results in nearly full reduction of $[N\text{-}2]_E$ within 17 s. In membrane particles pretreated with piericidin A, the cluster $[N\text{-}1]_E$ is only partly reducible by deamino-NADH and shows an altered line shape. The two remaining fast relaxing iron–sulfur clusters, $[N\text{-}3a]_E$ ($g_\perp = 1.94$, $g_\parallel = 2.02$) and $[N\text{-}3b]_E$ ($g_\perp = 1.94$, $g_\parallel = 2.03$), have an $E_{m7.4}$ of −260 mV ($n = 2$). These clusters may also be part of the NADH–Q oxidoreductase since in the mutant IY91, which possesses a very low level of deamino-NADH–Q oxidoreductase activity, they are modified in both their redox and spectral properties as is the $g_x = 1.90$ signal of the cluster $[N\text{-}2]_E$.

In *Escherichia coli*, the nature of the membrane-bound NADH–ubiquinone (Q) oxidoreductase (previously referred to as NADH dehydrogenase) and its role in the formation of a proton electrochemical gradient ($\Delta\tilde{\mu}_{H^+}$) have remained unresolved for many years. Early studies into the nature of the NADH dehydrogenase have indicated the presence of multiple enzymes with NADH dehydrogenase activity. In deoxycholate extracts from *E. coli* membrane particles, Bragg and Hou (1967) suggested the presence of two different NADH dehydrogenase enzymes on the basis of their substrate and inhibitor specificity. Gutman et al. (1968) studied a NADH dehydrogenase that was released from membrane particles by lyophilization and rehydration. They demonstrated the presence of non-heme iron and acid-labile sulfur as well as flavin in this preparation. Hendler and Burgess (1974)

† Supported by NIH Grant GM 30736 to T.O. and National Research Service Award GM 11165 to S.W.M.

* Author to whom correspondence should be addressed.

‡ University of Pennsylvania.

§ Roche Institute of Molecular Biology.

‖ Present address: Department of Agricultural Chemistry, Faculty of Agriculture, Yamaguchi University, Yamaguchi 753, Japan.

0006-2960/89/0428-2153$01.50/0